Thermodynamic Solution Model for Trona Brines

Henry W. Haynes, Jr.
Dept. of Chemical and Petroleum Engineering, University of Wyoming, Laramie, WY 82071

A thermodynamics solution model has been developed for concentrated trona brines over temperatures ranging from about 0°C to 200°C. The model was constructed by regressing on solubility data for the temperature-dependent parameters in Pitzer's activity coefficient model. In addition, the model incorporates published thermochemical data for the solid salts and aqueous species. In some cases it was necessary to estimate solid salt heat capacities, but otherwise no adjustments were made in the thermochemical parameters. With one exception, the model provided an excellent fit to the data. The existence of a high-temperature trona phase reported earlier cannot be reconciled with the model and is believed to be in error. The phase-equilibrium diagram generated by the model appears suitable for design purposes.

Introduction

The trona industry in southwestern Wyoming is North America's principal source of soda ash, and markets for Wyoming soda ash continue to expand into the Pacific Rim countries. Trona ore ($>90\%$ sodium sesquicarbonate, $Na_2CO_3 \cdot NaHCO_3 \cdot 2H_2O$) is mechanically mined at depths of up to 500 m and brought to the surface where it is processed into soda ash (anhydrous Na_2CO_3) and other sodium-based chemicals. Most soda ash is produced by the "monohydrate" process in which the raw trona ore is first calcined to decompose the bicarbonate ion. The crude soda ash product is then subjected to a crystallization purification process whereby sodium carbonate monohydrate crystals are formed. Upon removal of the water of hydration, a dense soda ash is produced. In the alternative "sesqui" process, the raw trona ore is first dissolved, and sodium sesquicarbonate is produced by crystallization. This material is then calcined to produce soda ash. In either case, purification and separation of the product are heavily dependent upon phase-equilibrium relationships that were developed from experiments conducted in the first half of the last century.

These empirical phase relationships have served the industry well. The natural-soda-ash industry has grown steadily since its inception in the early 1950s, and today over 20 million tons of trona are mined annually in the Green River Basin. Normally the process brines are almost entirely composed of sodium, carbonate, and bicarbonate ions. Traces of other soluble impurities can be handled with a purge stream. However, situations are sometimes encountered in which it becomes necessary to deal with foreign ions. For example, the tailings ponds associated with the mining and processing operations generally contain substantial amounts of sulfate. These ponds are potentially a valuable resource, but it will be necessary to deal with sulfate ions should it become desirable to process pond liquor. Similarly, solution-mined trona brines are known to contain chloride. While solubility data on mixed electrolytes are available in specific cases, the range of temperatures and compositions over which these contaminated brines can be processed is very wide. It sometimes becomes necessary to collect additional data to establish the necessary phase relationships. Alternatively, these relationships might be calculated from a thermodynamics-solution model.

The ultimate goal of the research described herein is to develop a thermodynamics-solution model that can be applied to mixed electrolytes over a wide range of compositions and temperatures. In the present communication, the system is limited to trona solutions at temperatures from the freezing point of water to 200°C. Earlier work on this system was limited to temperatures below 50°C (Peiper and Pitzer, 1982; Monnin and Schott, 1984), although we reported some preliminary results applicable to temperatures as high as 100°C (Haynes and De Filippis, 2000). In a subsequent contribution the results of this study will be coupled with high-temperature studies on other systems to make predictions of phase behavior and other thermodynamic equilibria in the presence of foreign ions.

Approach

The basis of these calculations will be molality-based solubility products for the various salts of interest. Thus, for the dissolution of sodium sesquicarbonate in pure water, we can write

$$\mathrm{Na_2CO_3 \cdot NaHCO_3 \cdot 2H_2O(s) \rightleftarrows 3Na^+(aq) + CO_3^=(aq) + HCO_3^-(aq) + 2H_2O(l)}$$

and the solubility product is given by

$$\begin{aligned} K_{sp} &\equiv \hat{a}^3_{\mathrm{Na^+}} \hat{a}_{\mathrm{CO_3^=}} \hat{a}_{\mathrm{HCO_3^-}} \hat{a}^2_w \\ &= (\gamma_{\mathrm{Na^+}} m_{\mathrm{Na^+}})^3 (\gamma_{\mathrm{CO_3^=}} m_{\mathrm{CO_3^=}})(\gamma_{\mathrm{HCO_3^-}} m_{\mathrm{HCO_3^-}}) \hat{a}^2_w \\ &= \gamma^3_{\mathrm{Na_2CO_3}} \gamma^2_{\mathrm{NaHCO_3}} m^3_{\mathrm{Na^+}} m_{\mathrm{CO_3^=}} m_{\mathrm{HCO_3^-}} \hat{a}^2_w \end{aligned} \tag{1}$$

where the γ_{MX} are mean ionic activity coefficients having the definition

$$\gamma^{\nu}_{MX} \equiv \gamma^{\nu_+}_M \gamma^{\nu_-}_X \tag{2}$$

for the salt $M_{\nu_+}X_{\nu_-}$, which dissociates into $\nu = \nu_+ + \nu_-$ ions. The solvent activity, $\hat{a}_w$, is related to the osmotic coefficient, ϕ, according to

$$\ln(\hat{a}_w) = -\frac{\phi \Sigma m_i}{55.51} \tag{3}$$

The standard state for the salts is the pure solid salt, the standard state for the solvent is pure liquid water, and the standard state for all ions in solution is the hypothetical 1-molal ideal solution (Henry's law sense). In all cases the standard-state temperature is system temperature and the standard-state pressure is taken as one bar (in some cases the standard-state pressure is the saturation pressure, but since we are dealing with condensed phases, the correction to one bar can be ignored).

Provided that the salts dissolve completely and that only sodium carbonate and sodium bicarbonate are present, the ion molalities in Eq. 1 can be calculated from the salt compositions using stoichiometry. Thus

$$\begin{aligned} m_{\mathrm{Na^+}} &= 2m_{\mathrm{Na_2CO_3}} + m_{\mathrm{NaHCO_3}} \\ m_{\mathrm{CO_3^=}} &= m_{\mathrm{Na_2CO_3}} \\ m_{\mathrm{HCO_3^-}} &= m_{\mathrm{NaHCO_3}} \end{aligned} \tag{4}$$

Here it is implicitly assumed that compositions are not altered significantly by homogeneous reaction equilibria, namely, the self-ionization of water and the first and second ionizations of carbonic acid. While the introduction of small amounts of hydroxyl ion and dissolved carbon dioxide by these reactions may be important in dilute solutions, saturated trona solutions are by their nature highly concentrated. Homogeneous reaction equilibria can thus be ignored. Another potential complication is ion association, which generally increases in importance at high temperatures and in concentrated solutions. The most likely candidate is the association between the monovalent sodium cation and the divalent carbonate anion to form a monovalent sodium carbonate ion, $\mathrm{NaCO_3}^-$. However, rather than treat association reaction equilibria explicitly, the approach employed here is to treat a weak ion association as a strong solution nonideality. The effect is implicitly taken into account by the activity coefficient model.

The solubility product is related to the standard Gibbs free energy of reaction according to the familiar relation

$$\ln(K_{sp}) = -\frac{\Delta G^o_{sp,T}}{RT} \tag{5}$$

Thus, the various solubility products can be obtained from thermochemical data for the salts, the solvent, and the ions in solution. The thermochemistry of the sodium carbonate–sodium bicarbonate system is quite well known. Berg and Vanderzee (1978) and Vanderzee (1982) have critically evaluated the salt properties. Thermochemical data for the aqueous species are taken from the extensive work of Helgeson and coworkers (Shock and Helgeson, 1988; Shock et al., 1989). The thermochemical data from these sources appear to be of sufficient quality that the calculated values of $\ln(K_{sp})$ can be treated as known quantities, at least initially, with no adjustment to obtain an improved fit to the solubility data.

Concentrated electrolytes generally form highly nonideal solutions, and several activity coefficient models are available for application to such systems. The ion-interaction model of Pitzer was chosen for this study because of its applicability to mixed electrolyte solutions and the fact that it has been successfully applied to solubility calculations for many salts at 25°C, including the sodium carbonate–sodium bicarbonate system (Harvie et al., 1984). The Pitzer model has also been successfully applied to a smaller number of systems at elevated temperatures as high as 300°C. Some examples are provided by Pitzer and coworkers for aqueous NaCl (Rogers and Pitzer, 1982; Pitzer et al., 1984), aqueous $\mathrm{Na_2SO_4}$ (Pabalan and Pitzer, 1988), and mixed electrolytes (Pabalan and Pitzer, 1987). Others have included solubility data in the evaluation of Pitzer coefficients at elevated temperatures (Møller, 1988; Greenberg and Møller, 1989). Like all semiempirical activity coefficient models, the Pitzer model contains unknown temperature-dependent parameters that must be regressed with experimental data.

To summarize, all quantities in Eq. 1 and like equations for the other salts are calculable with the exception of the activity coefficients. Solution compositions are readily obtained from stoichiometry under the assumption that homogeneous reactions and ion-association reactions can be ignored. Thermochemical data for the sodium carbonate–sodium bicarbonate system are assumed to be of a quality sufficient to obtain accurate phase equilibria. The only unknown quantities are the parameters that appear in Pitzer's activity coefficient model. Solubility data will be regressed for these parameters. High-quality solubility data are available from several sources at temperatures below 100°C, and limited data of lesser quality are available at temperatures up to 200°C.

Thermochemical Calculations

Vanderzee and his students (Berg and Vanderzee, 1978; Vanderzee, 1982) have made a very thorough evaluation of

Table 1. Thermochemical Data at 25°C for the Solid Salts

Compound	ΔH_f^o (kJ/mol)	S^o (J/mol·K)
$NaHCO_3(s)$	-948.952 ± 0.210	102.36 ± 0.80
$Na_2CO_3(s)$	$-1{,}129.178 \pm 0.260$	134.98 ± 0.84
$Na_2CO_3 \cdot H_2O(s)$	$-1{,}429.736 \pm 0.270$	168.11 ± 0.84
$Na_2CO_3 \cdot 7H_2O(s)$	$-3{,}199.48 \pm 0.90$	422.36 ± 1.50
$Na_2CO_3 \cdot 10H_2O(s)$	$-4{,}079.777 \pm 0.500$	562.74 ± 1.15
$Na_2CO_3 \cdot NaHCO_3 \cdot 2H_2O(s)$	$-2{,}682.11 \pm 0.44$	303.13 ± 1.70
$Na_2CO_3 \cdot 3NaHCO_3(s)$	$-3{,}984.03 \pm 0.80$	435.33 ± 2.50

Source: Berg and Vanderzee (1978); Vanderzee (1982).

Table 2. Standard-State Heat-Capacity Coefficients for the Solid Salts*

Compound	a	b	C_p^o
$NaHCO_3(s)$	44.893	0.14389	87.79
$Na_2CO_3(s)$	64.648	0.16008	112.38
$Na_2CO_3 \cdot H_2O(s)$	69.051	0.26725	148.73
$Na_2CO_3 \cdot 7H_2O(s)$	(198.365)	(0.77739)	(430.14)
$Na_2CO_3 \cdot 10H_2O(s)$	287.609	0.88083	550.23
$Na_2CO_3 \cdot NaHCO_3 \cdot 2H_2O(s)$	(169.037)	(0.37293)	(280.23)
$Na_2CO_3 \cdot 3NaHCO_3(s)$	(199.327)	(0.59175)	(375.76)

*C_p^o in J/mol·K; T in K.

thermochemical data for the solid salts. For ions and neutral species in solution, the extensive work of Helgeson and coworkers is accessed. Helgeson's work has culminated in a revision of the Helgeson–Kirkham–Flowers (HKF) "equation of state" (Helgeson et al., 1981; Tanger and Helgeson, 1988), which, however, is somewhat a misnomer, since HKF calculations apply only to species in their standard states. The only missing thermochemical data are standard-state heat capacities for some of the salt species. These have been estimated as described below.

Relevant thermochemical data for the salts of interest to this study were taken from Berg and Vanderzee (1978) and Vanderzee (1982) and are compiled in Table 1. In order to compute thermodynamic properties of these salts at elevated temperatures, standard-state heat capacities are required as a function of temperature. These data are available for anhydrous sodium carbonate, for sodium bicarbonate, and for the monohydrate and decahydrates of sodium carbonate.

Heat capacity data for sodium carbonate and sodium bicarbonate taken from the compilation of Chang and Ahmad (1982) were plotted vs. temperature over the range 298 to 500 K. A good straight line fit was obtained for both solids. For sodium carbonate the isobaric heat capacity in J/mol·K is given by

$$C_p^o = 64.648 + 0.16008T \tag{6}$$

where T is in K. Similarly for sodium bicarbonate

$$C_p^o = 44.893 + 0.14389T \tag{7}$$

Grønvold and Meisingset (1983) reported molar heat capacities for sodium carbonate monohydrate over the temperature range 250 to 380 K. Their data are in excellent accord with

$$C_p^o = 69.051 + 0.26725T \tag{8}$$

This same study also provided heat capacities for the decahydrate over the temperature range 298 to 305 K. Thus

$$C_p^o = 287.609 + 0.888083T \tag{9}$$

Note that heat-capacity data are needed only from the reference temperature ($T_r = 298.15$ K) to the maximum temperature that a particular salt can exist. Thus, the temperature ranges covered by the preceding expressions are adequate.

It appears that no heat-capacity data are available for the remaining salts—trona, Wegscheiderite, and sodium carbonate heptahydrate. These were estimated by assuming that ΔC_p^o is zero for the following formation reactions

$$Na_2CO_3(s) + NaHCO_3(s) + 2H_2O(hyd) = Na_2CO_3 \cdot NaHCO_3 \cdot 2H_2O(s)$$

$$Na_2CO_3(s) + 3NaHCO_3(s) = Na_2CO_3 \cdot 3NaHCO_3(s)$$

and

$$Na_2CO_3 \cdot 10H_2O(s) = 3H_2O(hyd) + Na_2CO_3 \cdot 7H_2O(s)$$

For the water of hydration, the heat capacity of "structural" water taken from Helgeson and coworkers (1978) was employed

$$C_p^o = 29.748 + 0.03448T \tag{10}$$

In summary, parameters in the general linear expression for heat capacity

$$C_p^o = a + bT \tag{11}$$

are compiled in Table 2. Those values in ( ) are estimated on the basis of the formation reactions as described. Standard-state heat capacities at the reference temperature (298.15 K) were calculated from the preceding expressions and entered into the last column of the table. In some cases, these values tend to be slightly higher than values recommended by Vanderzee, who also estimated C_p^o values for trona, Wegscheiderite, and the heptahydrate. Other small differences arise because the data of Grønvold and Meisingset were unavailable to Vanderzee, who based his calculations on the earlier heat-capacity data of Waterfield et al. (1968).

Thermochemical data for all aqueous species were obtained from the HKF model, which provides *apparent* standard Gibbs free energies of formation. The "apparent" standard Gibbs free energy differs from the *conventional* standard Gibbs free energy of formation in the following way: The "apparent" standard Gibbs free energy of formation of a component at any temperature is defined as the Gibbs free energy required to form one mole of the compound at specified temperature, T, from the elements *at the reference temperature ($T_r = 298.15$ K)*, all species in their standard states.

Table 3. Standard State Entropies at 25°C ($P^o = 1$ bar)

Element	S^o_{298} (J/mol·K)
Na(s)	51.30 ± 0.20
C(s)	5.74 ± 0.10
O_2(g)	205.152 ± 0.005
H_2(g)	130.680 ± 0.003

Source: Cox et al. (1989).

The "conventional" or "actual" standard Gibbs free energy of formation is referenced to the elements at *system temperature, T*. The following equation relates the apparent standard Gibbs free energy of formation of the salt to thermochemical parameters compiled in the preceding tables

$$\Delta G^{o,\mathrm{app}}_{f,T} = \Delta H^o_{f,298} - TS^o_{s,298} + a(T - T_r)$$
$$- \frac{1}{2} b(T - T_r)^2 - aT \ln(T/T_r) - T_r \sum_{j,\mathrm{elem}} \nu_j S^o_{j,298} \quad (12)$$

The last term is the sum over all the formation elements in their standard states. Thus, in order to compute apparent standard Gibbs free energies of formation for the various salts, the standard-state entropies of the elements at the reference temperature are required. Data from the CODATA task group (Cox et al., 1989) are compiled in Table 3.

Apparent standard Gibbs free energies of formation for all aqueous species and for the solvent, water, were calculated from the HKF model using parameters provided by Shock and coworkers (Shock and Helgeson, 1988; Shock et al., 1989). Tabulated values provided by Oelkers and coworkers (1995) were used as a check on the computations. The standard Gibbs free energy change for the dissolution reactions were calculated using

$$\Delta G^o_{sp,T} = \sum_j \nu_j \Delta G^{o,\mathrm{app}}_{f,T,j} \quad (13)$$

where the ν_j are now stoichiometric coefficients in the dissolution reaction for a particular salt.

Having computed the standard Gibbs free energy change for all the dissolution reactions, the solubility products were next calculated using Eq. 5. The results of these computations are presented in Figure 1. This figure displays the results of equilibrium calculations for all salts relevant to this study. In subsequent calculations, it will be convenient to have simple mathematical expressions for the equilibrium constants plotted in Figure 1. Accordingly, these computational results have been subjected to regression analysis using an equation of the form

$$\ln(K_{sp}) = B_1 T^{-1} + B_2 + B_3 \ln(T) + B_4 T + B_5 T^2$$

with T in K. The regression coefficients are compiled in Table 4. Equation 14 reproduces the results plotted in Figure 1 to two decimals in $\ln(K_{sp})$. Since the evaluation of these expressions may involve differences between large numbers, round-off of the coefficients is not recommended.

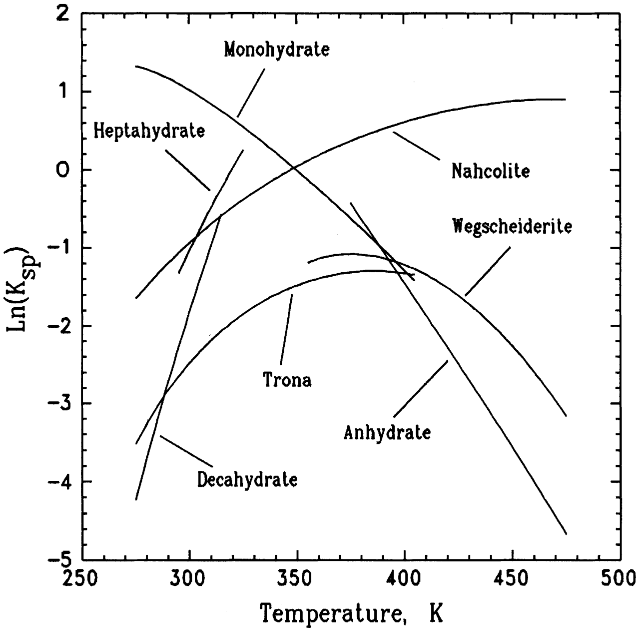

Figure 1. Ln(K_{sp}) values for various salts.

At low temperatures, slightly below 0°C because of the freezing-point depression, ice will form. Consider the equilibrium between solid and liquid water

$$H_2O(s) \rightleftarrows H_2O(l) \quad (V)$$

Taking the standard state as the pure liquid and pure solid, we can write

$$K_{\mathrm{fus}} = \frac{\hat{a}_{H_2O(l)}}{\hat{a}_{H_2O(s)}} = \hat{a}_w \quad (15)$$

Thus, the equilibrium constant for melting is equivalent to the activity of water. This equilibrium constant is related to the standard Gibbs free energy change according to Eq. 5, and upon substituting the definition of Gibbs free energy $\boldsymbol{G} \equiv \boldsymbol{H} - T\boldsymbol{S}$, we have

$$\ln(K_{\mathrm{fus}}) = \frac{\Delta S^o_T}{R} - \frac{\Delta H^o_T}{RT} \quad (16)$$

Over the small temperature range of interest (only about 3°C), it may be reasonably assumed that both ΔS^o and ΔH^o are constant, and these quantities are readily obtained from the steam tables (Keenan and Keys, 1936). Thus

$$\ln(K_{\mathrm{fus}}) = 2.6448517 - \frac{722.4412419}{T} \quad (17)$$

Activity Coefficient Model

According to Pitzer's ion-interaction theory, the excess

Gibbs free energy is written as a virial expansion, that is

$$\frac{G_m^E}{RT} = w_w f(I,T) + \frac{1}{w_w} \sum_j \sum_k \lambda_{jk}(I,T) n_j n_k + \frac{1}{w_w^2} \sum_j \sum_k \sum_l \mu_{jkl} n_j n_k n_l \quad (18)$$

where $f(I,T)$ is a Debye–Hückel term that accounts for long-range electrostatic forces, and $\lambda_{jk}(I,T)$ and μ_{jkl} are, respectively, the second and third virial coefficients that account for the effect of short-range interactions. The Debye–Hückel term is a function of ionic strength, I, and absolute temperature, and can be calculated from theory. The second virial coefficients, also functions of ionic strength and temperature, are empirical parameters. Similarly, the third virial coefficients are empirical parameters that generally assume lesser importance by comparison to the second virial coefficients. They may often be treated as constants or simply ignored. The molality-based ionic strength has the usual definition

$$I \equiv \frac{1}{2} \sum_j m_j z_j^2 \quad (19)$$

where z_j is the charge on the jth ion.

Pitzer (1995) shows how Eq. 18 can be rearranged by imposing the condition of electrical neutrality and reasonable simplifying assumptions to obtain certain allowable groupings of the virial coefficients. The operation effectively reduces the number of model parameters. Since details are available in the preceding reference, only the working equations will be presented here.

The mean ionic activity coefficient for the salt $M_{\nu^+} X_{\nu^-}$ is given by the following expression

$$\begin{aligned} \ln \gamma_{MX} = & - z_M z_X \left\{ \frac{1}{2} f' + \sum_{i=1}^{n_c} \sum_{j=i+1}^{n_a} m_i m_j B'_{ij} + \sum_{i=1}^{n_c} \sum_{j=1}^{n_a} m_i m_j \Phi'_{ij} \right. \\ & \left. + \sum_{i=1}^{n_a} \sum_{j=i+1}^{n_a} m_i m_j \Phi'_{ij} \right\} + \frac{\nu_M}{\nu} \sum_{j=1}^{n_a} m_j \left(2B_{Mj} + ZC_{Mj} + 2\frac{\nu_X}{\nu_M} \Phi_{Xj} \right) \\ & + \frac{\nu_X}{\nu} \sum_{i=1}^{n_c} m_i \left(2B_{iX} + ZC_{iX} + 2\frac{\nu_M}{\nu_X} \Phi_{Mi} \right) \\ & + \frac{1}{\nu} \sum_{i=1}^{n_c} \sum_{j=1}^{n_a} m_i m_j \left(2\nu_M z_M C_{ij} + \nu_M \Psi_{Mij} + \nu_X \Psi_{ijX} \right) \\ & + \frac{\nu_X}{\nu} \sum_{i=1}^{n_c} \sum_{j=i+1}^{n_c} m_i m_j \Psi_{ijX} + \frac{\nu_M}{\nu} \sum_{i=1}^{n_a} \sum_{j=i+1}^{n_a} m_i m_j \Psi_{Mij} \quad (20) \end{aligned}$$

and for the osmotic coefficient

$$\begin{aligned} \phi = 1 + & \frac{2}{\sum_i m_i} \left\{ -\frac{1}{2}(f - If') + \sum_{i=1}^{n_c} \sum_{j=1}^{n_a} m_i m_j \left(B_{ij} + IB'_{ij} \right. \right. \\ & \left. + ZC_{ij} \right) + \sum_{i=1}^{n_c} \sum_{j=i+1}^{n_c} m_i m_j \left(\Phi_{ij} + I\Phi'_{ij} + \sum_{k=1}^{n_a} m_k \Psi_{ijk} \right) \\ & \left. + \sum_{i=1}^{n_a} \sum_{j=i+1}^{n_a} m_i m_j \left(\Phi_{ij} + I\Phi'_{ij} + \sum_{k=1}^{n_c} m_k \Psi_{kij} \right) \right\} \quad (21) \end{aligned}$$

where

$$Z \equiv \sum_{i=1}^{n_c} m_i z_i - \sum_{i=1}^{n_a} m_i z_i \quad (22)$$

For sums over n_c cations, the m_i represent cation molalities, and likewise for sums over n_a anions, the m_i represent anion molalities. Computation of the various functions appearing in Eqs. 20 and 21 will be addressed next.

The Debye–Hückel term, f, is a modification of the original Debye–Hückel limiting law. Pitzer (1995) writes

$$f = -\frac{4Ia}{b} \ln(1 + bI^{1/2}) \quad (23)$$

Here, the parameter a is a temperature-dependent parameter equal to one-third the original Debye–Hückel parameter. Its value at 25°C is $a = 0.3915\ \mathrm{kg}^{1/2} \cdot \mathrm{mol}^{-1/2}$. The expression of Møller (1988), valid for temperatures from 0°C to 300°C, was employed in this study. The parameter b is assigned a universal value of $b = 1.2\ \mathrm{kg}^{1/2} \cdot \mathrm{mol}^{-1/2}$. The derivative of the modified Debye–Hückel function, Eq. 23, is given by

$$f' \equiv \frac{df}{dI} = \frac{f}{I} - \left(\frac{2aI^{1/2}}{1 + bI^{1/2}} \right) \quad (24)$$

It is a simple matter to show that these equations reduce to the original Debye–Hückel limiting law in the infinite dilution limit.

The quantity, B_{ij}, in Eqs. 20 and 21 is a collection of second virial coefficients, that is, the λ_{ij} of Eq. 18, which accounts for two-way interactions between ions of unlike sign, that is, between cations and anions. In isothermal systems, Pitzer recommends the following semiempirical equation for the ionic strength dependence of the B_{ij}

$$B_{ij} = \beta_{ij}^{(0)} + \beta_{ij}^{(1)} g\left(\alpha_1 I^{1/2} \right) \quad (25)$$

This expression is suitable for 1–1 (such as NaCl), 2–1 (such as $MgCl_2$), and 1–2 (such as Na_2SO_4) -type electrolytes with $\alpha_1 = 2.0\ \mathrm{kg}^{1/2} \cdot \mathrm{mol}^{-1/2}$ (Pabalan and Pitzer (1988) employed a value of $\alpha_1 = 1.4\ \mathrm{kg}^{1/2} \cdot \mathrm{mol}^{-1/2}$ for Na_2SO_4 for consistency with the earlier work of Holmes and Mesmer (1986). They report only a "slight improvement" with this modification of the original Pitzer formulation. Consequently, the current calculations are based on $\alpha_1 = 2.0\ \mathrm{kg}^{1/2}\cdot\mathrm{mol}^{-1/2}$). The function $g(x)$ is given by

$$g(x) \equiv \frac{2[1-(1+x)e^{-x}]}{x^2} \qquad (26)$$

For 2–2 (such as $MgSO_4$) -type electrolytes, α_1 is shifted, and an additional term is needed in Eq. 25. Thus, for 2–2-type electrolytes

$$B_{ij} = \beta_{ij}^{(0)} + \beta_{ij}^{(1)} g\left(\alpha_1 I^{1/2}\right) + \beta_{ij}^{(2)} g\left(\alpha_2 I^{1/2}\right) \qquad (27)$$

where $\alpha_1 = 1.4\ \mathrm{kg}^{1/2}\cdot\mathrm{mol}^{-1/2}$ and $\alpha_2 = 12\ \mathrm{kg}^{1/2}\cdot\mathrm{mol}^{-1/2}$. The ionic strength derivative function, B'_{ij}, is also required. Differentiation of the previous equation provides

$$B'_{ij} \equiv \frac{\partial B_{ij}}{\partial I} = \alpha_1^2 \beta_{ij}^{(1)} \left[\exp\left(-\alpha_1 I^{1/2}\right) - g\left(\alpha_1 I^{1/2}\right)\right] \left(\alpha_1 I^{1/2}\right)^{-2} + \alpha_2^2 \beta_{ij}^{(2)} \left[\exp\left(-\alpha_2 I^{1/2}\right) - g\left(\alpha_2 I^{1/2}\right)\right] \left(\alpha_2 I^{1/2}\right)^{-2} \qquad (28)$$

Common practice is to use these same functions at elevated temperatures, and to correlate the β_{ij} coefficients with temperature.

The Φ_{ij} are also collections of second virial coefficients, but unlike the B_{ij}, they represent interactions between ions of like sign. They consist of two terms, that is

$$\Phi_{ij} = \theta_{ij} + {}^{E}\theta_{ij} \qquad (29)$$

with the former, θ_{ij}, being independent of ionic strength. The second term, ${}^{E}\theta_{ij}$, on a complex manner upon ionic strength, but disappears for symmetrical mixing. Thus θ_{ij} is a fitting parameter independent of ionic strength, and ${}^{E}\theta_{ij}$ is computed as follows. Define

$$x_{ij} = 6 z_i z_j a I^{1/2} \qquad (30)$$

where a is the modified Debye–Hückel parameter introduced earlier. The ${}^{E}\theta_{ij}$ are related to the x_{ij} according to

$${}^{E}\theta_{ij} = \frac{z_i z_j}{4I}\left[J(x_{ij}) - \frac{1}{2}J(x_{ii}) - \frac{1}{2}J(x_{jj})\right] \qquad (31)$$

and the J-functions are given by

$$J(x) = x\left[4 + 4.581 x^{-0.7237} \exp\left(-0.012 x^{0.528}\right)\right]^{-1} \qquad (32)$$

For the derivatives

$$\Phi'_{ij} = {}^{E}\theta'_{ij} \equiv \frac{d\,{}^{E}\theta_{ij}}{dI} \qquad (33)$$

and

$${}^{E}\theta'_{ij} = -\frac{{}^{E}\theta_{ij}}{I} + \frac{z_i z_j}{8I^2}\left[x_{ij} J'(x_{ij}) - \frac{1}{2} x_{ii} J'(x_{ii}) - \frac{1}{2} x_{jj} J'(x_{jj})\right] \qquad (34)$$

where

$$J' \equiv \frac{dJ}{dx} = \frac{J}{x} + \left(\frac{J}{x}\right)^2 \left[3.3152697 x^{-0.7237} + 0.029025216 x^{-0.1857}\right] \exp\left(-0.012 x^{0.528}\right) \qquad (35)$$

The quantities C_{ij} and Ψ_{ijk}, which appear in Eqs. 20 and 21, are collections of third virial coefficients (the parameter, $C_{ij} = C_{ji}$, is composed of third virial coefficients for common cations and common anions; hence, only two subscripts are needed), that is, the μ_{ijk} of Eq. 18, and as such they tend to be of lesser importance compared to the B_{ij} and Φ_{ij}. In many cases acceptable results can be obtained by ignoring these terms.

In summary, the following parameters are required to characterize a multicomponent mixture of strong electrolytes

$\beta_{ij}^{(0)}$
$\beta_{ij}^{(1)}$—One value for each cation–anion pair;
$\beta_{ij}^{(2)}$
θ_{ij}—One value for each cation–cation pair, and one value for each anion–anion pair;
C_{ij}—One value for each cation–anion pair;
Ψ_{ijk}—One value for each cation–cation–anion triplet, and one value for each anion–anion–cation triplet.

Note that the β_{ij} are in essence single electrolyte parameters, since only single cation–anion interactions are involved. The θ_{ij}, on the other hand, may be considered mixing parameters, since they arise only in multiple electrolytes systems, that is, systems in which multiple cations and/or multiple an-

Table 4. Coefficients for Eq. 14 for Solubility Products

Compound	B_1	B_2	B_3	B_4	$B_5 \times 10^4$
$NaHCO_3(s)$	−15,577.51	580.2894	−105.8717	0.2924303	−1.461392
$Na_2CO_3(s)$	−70,816.77	2,919.663	−529.0907	1.290843	−5.648249
$Na_2CO_3\cdot H_2O(s)$	−63,465.90	2,851.752	−528.8011	1.472089	−7.181693
$Na_2CO_3\cdot 7H_2O(s)$	−18,934.49	484.9108	−80.11826	0.1138303	0
$Na_2CO_3\cdot 10H_2O(s)$	−37,806.14	1,165.010	−200.0793	0.3346646	0
$Na_2CO_3\cdot NaHCO_3\cdot 2H_2O(s)$	−87,930.46	3,786.877	−701.5103	1.973255	−9.662326
$Na_2CO_3\cdot 3NaHCO_3(s)$	−120,952.7	4,776.029	−868.0586	2.226852	−10.29110

ions are present. Studies at elevated temperatures have clearly demonstrated that the β_{ij} are temperature dependent. However, it remains to be determined whether the remaining parameters can be assumed to be independent of temperature.

Critical Survey of Solubility Data

Solubility data for the Na_2CO_3-$NaHCO_3$-H_2O system over temperatures ranging from 0°C to 200°C were obtained from several sources including Freeth (1922) at 0°, 15°, 20°, 25°, 30°, 35°, 45°, and 60°C; Hill and Bacon (1927) at 24.87°, 30°, and 50°C; Wegscheider and Mehl (1928) at 20°, 22°, 25.9°, 30°, 39.9°, 49.7°, 69.7°, 79.6°, 84.6°, 89.5°, and 94.5°C, Waldeck and coworkers (1934) at 100°, 150°, 170°, 190°, and 200°C; and Tomaszewski (1961) at 50°C. In addition, solubility data for pure Na_2CO_3 and $NaHCO_3$, critically evaluated and compiled by Linke (1965), were included in the database. In some cases, where there were obvious inconsistencies in the data, the points in question were removed from the data set. For example, Harvie and coworkers (1984) have already pointed out some inconsistencies in Freeth's 25°C data. Similarly, there appears to be a typographical error in the 100°C data of Waldeck and coworkers. In both cases the points in question were eliminated. The study of Wegscheider and Mehl identified a suspected solid "trisalz" ($Na_2CO_3 \cdot 3NaHCO_3 \cdot xH_2O$) phase and possibly a "disalz" ($Na_2CO_3 \cdot 2NaHCO_3 \cdot 2H_2O$) in their system. The trisalt is now known as Wegscheiderite ($x = 0$), but there has been no further evidence to support the formation of the disalt. These investigators report the presence of what evidently are metastable nahcolite and trona phases in regions where the less soluble Wegscheiderite forms. Since the existence of Wegscheiderite has now been firmly established in these high-temperature systems, these metastable nahcolite and trona points were omitted from the database. This occurred in the 89.5°C and 94.5°C isotherms. Such points aside, there are still ample high-quality data available at temperatures below 100°C to ensure a high confidence in the regression analysis. Since only single-source data are available at temperatures above 100°C, there is less confidence in this region.

Evaluation of Model Parameters

In general, the model parameters were obtained by minimizing the sum of squares of deviations between the theoretical and calculated values of $\ln(K_{sp})$ for each salt. The theoretical values were obtained from Eq. 14 and the parameters of Table 4. The calculated values of $\ln(K_{sp})$ were obtained from definitions of the various solubility products in terms of activities or activity coefficients and composition. For example, the calculated $\ln(K_{sp})$ for trona is obtained from Eq. 1 after taking logarithms. Thus

$$\ln(K_{sp})|_{\text{calc}} = 3\ln(\gamma_{Na_2CO_3}) + 2\ln(\gamma_{NaHCO_3}) + 3\ln(m_{Na}) + \ln(m_{CO_3}) + \ln(m_{HCO_3}) + 2\ln(\hat{a}_w) \quad (36)$$

Similar expressions were written for the other salts. The objective function is then

$$\Phi \equiv \sum \left[\ln(K_{sp}) - \ln(K_{sp})|_{\text{calc}}\right]^2 \quad (37)$$

where the sum is taken over all the data, and the appropriate $\ln(K_{sp})$ value is selected for the salt corresponding to the particular datum. The Pitzer model parameters are contained in the activity coefficients, as already discussed.

The problem is thus reduced to finding the set of model parameters that minimizes Φ. This is no small task given the fact that the model is highly nonlinear, and iterative means must therefore be employed to find the minimum. Good success was achieved using the Nelder−Mead optimization method as described by Riggs (1988), and his code was modified for use in the current problem. The computation procedure proved to be very robust, although it was slow.

It is generally difficult to make statistical inferences in nonlinear regressions of the type undertaken here. The model parameters tend to be biased and nonnormally distributed. However, as sample size increases, these difficulties ultimately disappear, and in the "asymptotic" (that is, large n) case, one can use the usual test statistics employed in linear regression analysis. For the very large data set ($n > 500$), which formed the basis of this analysis, the following F-test was employed to test the significance of one or more deleted variables

$$F_\alpha(p - p^*, n - p) = \frac{(SSE^* - SSE)/(p - p^*)}{SSE/(n - p)} \quad (38)$$

where SSE is the error sum of squares and p is the number of model parameters. Those quantities with the asterisk are with the variable(s) in question deleted. This test proved very useful in evaluating the significance of the regression parameters.

A series of preliminary isothermal regressions was performed to explore the relative significance of the various Pitzer parameters, and also to obtain a qualitative determination of the temperature dependence of the parameters that appeared to be significant. A subset of the total database was employed that included individual isotherms over the entire temperature range (0°C to 200°C). An analysis along these lines that, however, was limited to a maximum temperature of 100°C, was reported earlier (Haynes and De Filippis, 2000). Generally it was found that reasonable fits to a particular isotherm could be obtained using only the four single electrolyte parameters: $\beta^{(0)}_{Na,CO_3}$, $\beta^{(1)}_{Na,CO_3}$, $\beta^{(0)}_{Na,HCO_3}$, and $\beta^{(1)}_{Na,HCO_3}$. No improvement in the fit could be realized by including any of the third virial-coefficient terms; nor was it necessary at this stage to include the interaction parameter, θ_{CO_3,HCO_3}.

The parameter set obtained at each temperature was next subjected to regressions with empirical temperature functions. It was found that both $\beta^{(0)}$ terms were only mildly temperature dependent, if at all. However, the $\beta^{(1)}$ terms exhibited a strong temperature dependence, and in the case of the asymmetric combination (Na^+−$CO_3^=$), the temperature dependence was rather complex. After experimenting with numerous functional forms for the temperature depen-

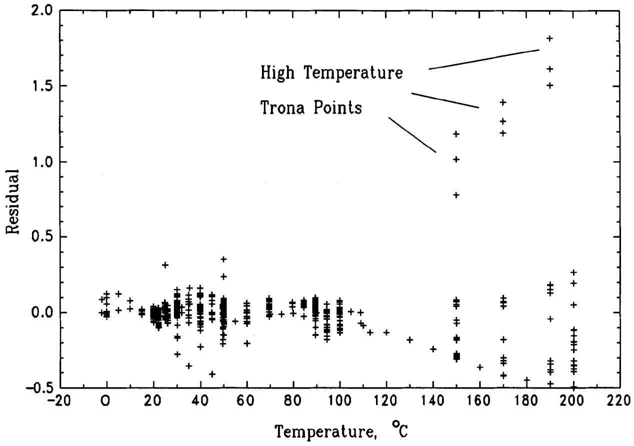

Figure 2. Residuals plot for base-case regression, Eq. 39, on entire data set: $n = 552$, $Lp = 12$, SSE = 22.612555.

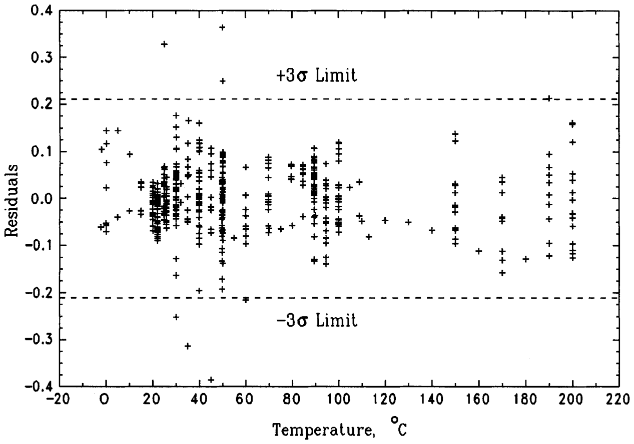

Figure 3. Residuals plot for base-case regression, Eq. 39, on data set with high-temperature trona points removed: $n = 543$, $p = 12$, SSE = 2.624985.

dence of these coefficients, the following expressions were found to perform well over the entire temperature range covered by the study

$$
\begin{aligned}
T' &= T - b_1 \\
\beta^{(0)}_{\mathrm{Na,CO_3}} &= b_2 + b_3 T' \\
\beta^{(1)}_{\mathrm{Na,CO_3}} &= b_4(1 - e^{-b_5 T'}) + b_6 (T')^{b_7} e^{-b_8 T'} \\
\beta^{(0)}_{\mathrm{Na,HCO_3}} &= b_9 \\
\beta^{(1)}_{\mathrm{Na,HCO_3}} &= b_{10} + b_{11} T' + b_{12} (T')^2 \qquad (39)
\end{aligned}
$$

Originally, polynomial regressions were assumed for the temperature dependence of $\beta^{(1)}_{\mathrm{Na,CO_3}}$. However, it was necessary to call upon higher-order polynomials, which ultimately caused problems with convergence to local optima. The complex function for $\beta^{(1)}_{\mathrm{Na,CO_3}}$ was superior to a sixth-order polynomial, and it contains two less parameters (five vs. seven for the polynomial fit).

Results

The entire data set (after the removal of inconsistent data, as discussed earlier) was next subjected to a regression in which the twelve parameters in Eq. 39 were adjusted to minimize the objective function Φ defined by Eq. 37. The residuals are plotted vs. temperature in Figure 2. The nine points identified as "high temperature trona points" on the figure are clearly responsible for the greatest portion of the regression error. These data are from Waldeck and coworkers (1934), who reported a stable trona phase at temperatures as high as 195°C. Scrutiny of the original article reveals that difficulties were experienced in achieving equilibrium in their unstirred equilibrium cell. They report that "satisfactory results on the trona curve could not be obtained by use of mixtures of the two components" (Na_2CO_3 and $NaHCO_3$), but the problem could be eliminated by charging the cell with "pure crystallized trona." The inconsistent behavior of these data, coupled with the Waldeck's inability to approach equilibrium from the forward direction strongly suggests that the assertion of a high-temperature trona phase is invalid. It appears that only one author (Tomaszewski, 1961) has included the high-temperature trona phase in his hand-drawn equilibrium phase diagram, but the existence of a high-temperature trona phase is inconsistent with published phase diagrams widely accepted by the trona industry (for example, Garrett, 1992). Accordingly, the points in question were removed from the data set.

With the high-temperature trona data removed, the regression was repeated, and a plot of the residuals is provided in Figure 3. Clearly, the fit to the model is much improved. Also shown on this figure are the $\pm 3\sigma$ limits on the mean regression line. For a normal distribution of errors, the probability that a point will lie outside these limits is about 0.002. Thus, for a data set of roughly 500 points, no more than one or two points should fall outside the $\pm 3\sigma$ limits. As shown in Figure 3, a number of points, eight to be exact, fall outside the limits. In every case but one, these points were associated with an isothermal invariant point corresponding to two solid phases in equilibrium with saturated solution. The larger experimental errors are probably associated with the experimental difficulty in locating these points. Accordingly, these eight "outlier" points were omitted from the data set and from subsequent analysis.

With this last operation, the effort to improve the quality of the database by identifying and removing questionable points was complete. The remaining total of 535 data points were next subjected to stepwise regressions with the aim to improve the model by deleting statistically insignificant terms, or by adding additional statistically significant terms. In each step one or more parameters were either added or removed, the entire regression was repeated, and the "extra sum of squares" due to the particular parameter(s) was tested for significance. The error sum of squares associated with various parameters is summarized in Table 5. The corresponding F-values were obtained from Eq. 38. Those calculated F-values identified by an asterisk (*) are significant compared to the critical $F_{0.05}(1, \infty) = 3.84$ for a single parameter or $F_{0.05}(2,$

Table 5. Extra Sum-of-Squares Analysis for Significance of Terms in Eq. 39 and Attempted Improvements

Source	*SSE*	*F*
Base case, Eq. 39	1.758288	—
Linear term in $\beta^{(0)}_{Na,CO_3}$	2.165491	121.1*
Quadratic term in $\beta^{(0)}_{Na,CO_3}$	1.758043	0.1
Constant $\beta^{(0)}_{Na,HCO_3}$	1.880556	36.4*
Linear term in $\beta^{(0)}_{Na,HCO_3}$	1.744933	1.74
Quadratic term in $\beta^{(1)}_{Na,HCO_3}$	2.872468	331.4*
Cubic term in $\beta^{(1)}_{Na,HCO_3}$	1.755737	0.76
Constant interaction term, θ_{CO_3,HCO_3}	1.755757	0.75
Temperature-dependent interaction term, θ_{CO_3,HCO_3}	1.704378	8.24*

*Significant parameters.

Table 6. Regressed Eqs. 39 and 40 Parameters

Parameter	Value	Parameter	Value
$b_1 \times 10^{-2}$	2.60369	$b_8 \times 10^2$	7.351792
$b_2 \times 10^2$	7.585726	$b_9 \times 10^3$	−9.306555
$b_3 \times 10^4$	−1.645319	b_{10}	−0.1093949
b_4	4.912421	$b_{11} \times 10^3$	8.39351
$b_5 \times 10^3$	3.656319	$b_{12} \times 10^5$	−1.863198
$b_6 \times 10^9$	4.097589	$b_{13} \times 10^3$	1.587083
b_7	5.68999	$b_{14} \times 10^5$	8.93501

$\infty) = 3.00$ for two parameters. The parameters b_4 to b_8 in Eq. 39 were not tested since no reasonable convergence could be obtained with any of these parameters omitted. The conclusions from this analysis are first that all terms in the base model, Eq. 39, are significant, and further that the inclusion of additional terms cannot be justified by the data. However, the correlation is significantly improved by including the temperature-dependent interaction parameter

$$\theta_{CO_3^{=},HCO_3^{-}} = b_{13} + b_{14}T' \tag{40}$$

A residuals plot for this model is provided in Figure 4. There is no obvious trend in the residuals with temperature. A normal scores plot of these residuals produced a good straight line except for a small deviation in the large negative residuals. The residuals are, thus, normally distributed. Regression parameters are compiled in Table 6.

Some representative calculated isotherms are compared with the data in Figure 5. Keep in mind that these are not curve fits to individual isotherms, but rather the regression is on the entire data set, which includes experimental results from numerous sources at many different temperatures. When viewed as a whole, the calculated results are probably comparable to the uncertainty in the data. Not surprisingly, the greatest misfit is in the 200°C isotherm. Although not shown, the calculated 190°C isotherm exhibits similar disparity when compared with the data. For reasons discussed previously, the high-temperature data of Waldeck and coworkers (1934) appears to be of rather poor quality. Thus, the inability of the model to provide a close fit to the 190°C and 200°C data may be as much a reflection of uncertainty in the data as of uncertainty in the model. Regardless, a note should be made of this discrepancy until the question is ultimately resolved by the attainment of additional high-temperature solubility data.

Phase-equilibrium diagrams calculated from the model are presented in Figures 6 and 7 for $T \leq 100°C$ and in Figure 8 for the high-temperature region. Invariant points are compiled in Table 7. (According to the phase rule, there is a single degree of freedom for three coexisting solid phases. Specifying pressure makes these points invariant.) The calculated phase diagrams are in good general agreement with phase diagrams that appear in the book by Garrett (1992). Small differences are evident, but as a matter of fact there are similar small discrepancies between Garrett's high-temperature ($T \leq 200°C$) and low temperature ($T \leq 100°C$) plots. Phase diagrams ($T \leq 100°C$) employed by the various companies operating in the Green River trona region also exhibit small discrepancies. In some cases, the phase relationships employed by industry may be based in part on proprietary data.

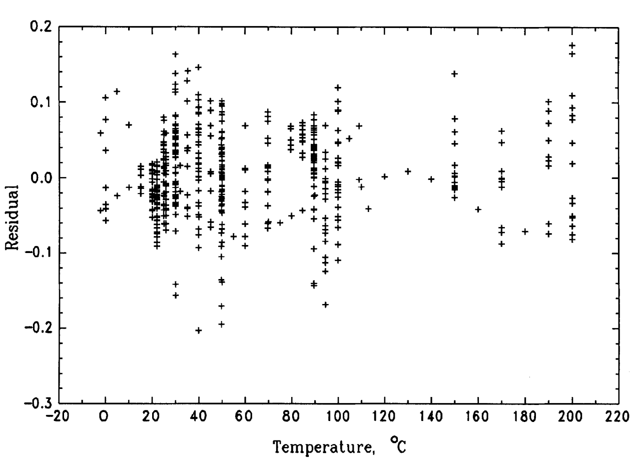

Figure 4. Residuals plot for model regression on reduced data set: $n = 535$, $p = 14$, SSE = 1.704378.

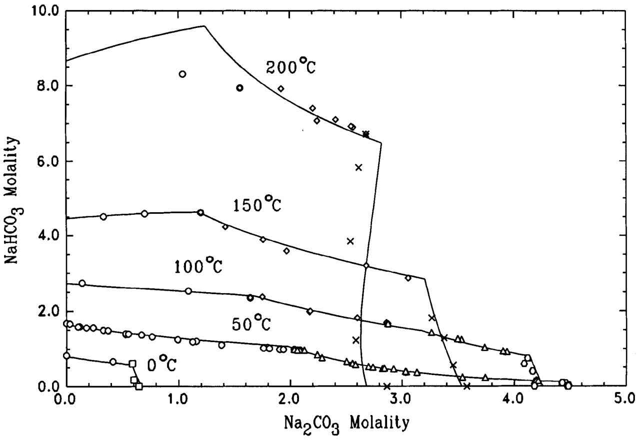

Figure 5. Selected calculated isotherms (lines) compared with the experimental data (points): ○—nahcolite; □—decahydrate; △—trona; ◇—wegscheiderite; ×—anhydrate.

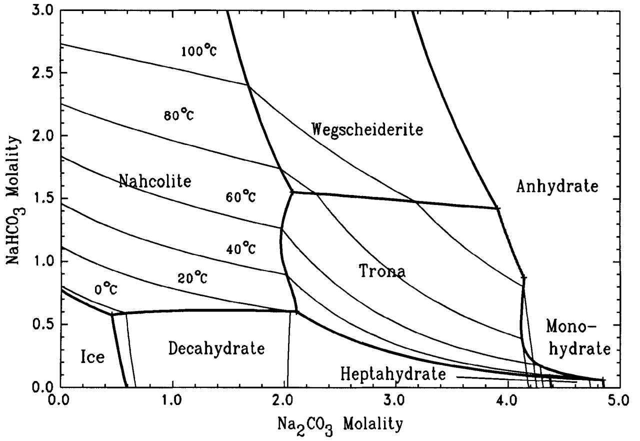

Figure 6. Trona-phase equilibrium diagram; low-temperature region.

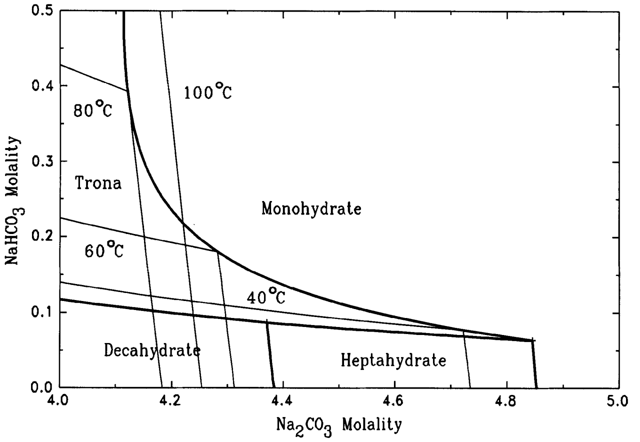

Figure 7. Trona-phase equilibrium diagram; detail for sodium carbonate heptahydrate region.

When studying phase diagrams from various sources, it is evident that the location of the nahcolite–trona–Wegscheiderite invariant point seems to vary over a fairly wide range (by some 15°C or more). Similar discrepancies are observed in the trona–Wegscheiderite–anhydrate invariant point. Generally, the model calculations fall within the extremes of phase diagrams that are widely employed by the trona industry. The model calculations would thus appear to be suitable for design purposes.

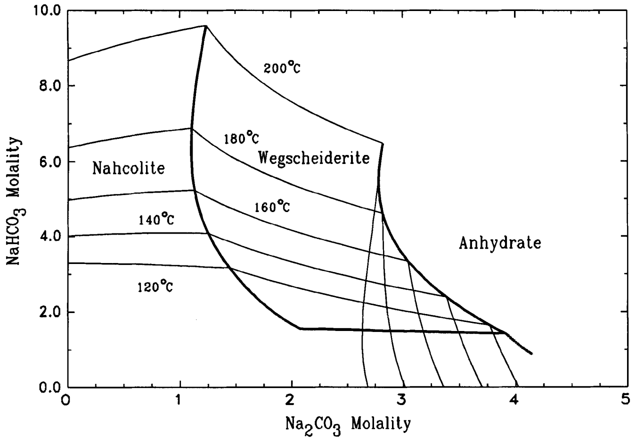

Figure 8. Trona-phase equilibrium diagram; high-temperature region.

Table 7. Calculated Invariant Points

Solid Phases	Na_2CO_3 Molality	$NaHCO_3$ Molality	T (°C)
Nahcolite–ice–decahydrate	0.46	0.58	−3.37
Nahcolite–decahydrate–trona	2.11	0.60	20.5
Trona–heptahydrate–decahydrate	4.37	0.087	32.3
Trona–monohydrate–heptahydrate	4.84	0.064	35.6
Nahcolite–trona–Wegscheiderite	2.08	1.55	73.7
Monohydrate–trona–anhydrate	4.14	0.87	102.4
Trona–Wegscheiderite–anhydrate	3.91	1.43	112.5

Discussion

It was pointed out earlier that solution compositions may be altered due to homogeneous reactions responsible for the production of H^+(aq), OH^-(aq), and CO_2(aq). These reactions were not considered to be an important factor in concentrated solutions, and the effect was ignored. However, when dealing with dilute solutions, the compositions of these components might be comparable in magnitude to the dissolved salt species. Thus, for computations on dilute systems it may be necessary to take into account additional equilibria for the hydrolysis of carbonate ion

$$CO_3^{=}(aq) + H_2O(l) \rightleftarrows HCO_3^{-}(aq) + OH^{-}(aq) \quad \text{(VI)}$$

and for the decomposition of bicarbonate

$$2HCO_3^{-}(aq) \rightleftarrows CO_3^{=}(aq) + CO_2(aq) + H_2O(l) \quad \text{(VII)}$$

Upon taking note of the strongly basic nature of trona brines, the hydrogen ion composition may be safely assumed to be zero, even in dilute solutions.

Equilibrium calculations based on the HKF model reveal that the thermodynamics of both of the preceding reactions strongly favors reactants at low temperatures. Further, the second reaction, responsible for the formation of aqueous CO_2, is unlikely to be significant at all temperatures covered by this investigation. The exclusion of aqueous CO_2 from the analysis of solubility data thus appears reasonable. The formation of hydroxyl ion begins to assume a small and possibly significant role at the higher temperatures. This said, it is unlikely that the formation of hydroxyl ion could be a significant factor in highly concentrated, saturated solutions.

The temperature dependencies of the Pitzer β-functions are provided in Figure 9. The $\beta^{(1)}$ term for sodium carbonate exhibits a clear hump, whereas, the temperature dependence of the analogous sodium bicarbonate term is much more gradual. These are empirical temperature functions, and one should not make too much ado over their shape. It is nevertheless tempting to suggest that the complex temperature dependence of the sodium carbonate parameter might

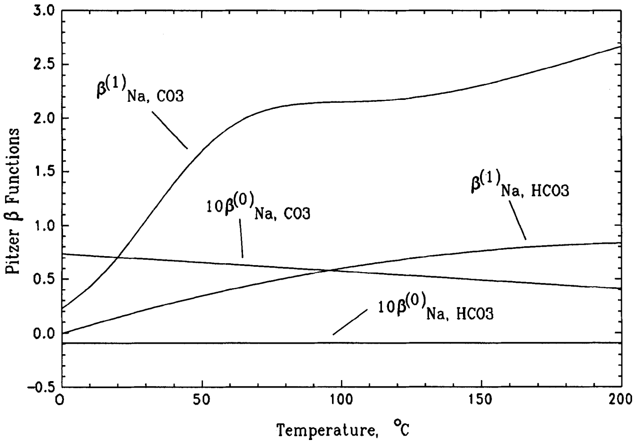

Figure 9. Temperature dependence of the regressed Pitzer β-functions.

be associated with the formation of the monovalent sodium carbonate ion, $NaCO_3^-$. Experimental evidence suggests that the monovalent sodium carbonate ion, $NaCO_3^-$, may be formed in this system (Garrels et al., 1961; Butler and Huston, 1970; Nakayama, 1971; Chen et al., 1992). However, attempts to obtain a significantly improved regression by explicitly including this component in the analysis were unsuccessful.

In the development of this model, it has not been necessary to adjust any thermochemical parameters. However, there is always considerable uncertainty in K_{sp} values, and under the best of circumstances, $\ln(K_{sp})$ values can only be calculated to within about one logarithmic unit when using thermochemical data from various sources. Higher accuracies, to within about a 0.2 logarithmic unit, are claimed when all calculations are based entirely on the HKF model, since internal consistency is assured (Oelkers et al., 1995). Thus, there would appear to be a potential for further improvement by allowing the solubility products to vary. Indeed, a small, but statistically significant improvement was obtained by allowing for a linear variation in $\ln(K_{sp})$ with temperature. The maximum adjustments to $\ln(K_{sp})$ varied from 0.28 to 0.59 for the various salts, and were thus well within the allowable range. However, these results are not reported here because of uncertainty in the high-temperature solubility data that was responsible for much of the adjustment.

Conclusions

A thermodynamic-solution model applicable to concentrated trona brines has been successfully constructed, which covers the temperature range from about 0°C to 200°C. The trona phase cannot exist above the trona-Wegscheiderite-anhydrate invariant point at about 113°C. Although some uncertainty is evident at the higher temperatures due to a lack of quality data in this region, phase-equilibrium diagrams generated from this model appear suitable for design calculations. The availability of Pitzer parameters for concentrated sodium carbonate/bicarbonate systems now makes it possible to explore the behavior of saturated mixed electrolyte systems of the type encountered in the trona industry.

Acknowledgments

The author gratefully acknowledges the financial support provided by the State of Wyoming through the Science, Technology and Energy Authority. Mr. Marco Germani and Prof. Paolo De Filippis of the University of Rome "La Sapienza" contributed significantly to this work in its early stages.

Notation

a = parameter in standard-state heat capacity, Eq. 11; modified Debye–Hückel parameter, Eq. 23
$\hat{a}_i$ = component activity, mol/kg
b = parameter in standard-state heat capacity, Eq. 11; modified Debye–Huckel parameter, Eq. 23; regression coefficient
B = parameter in Eq. 14
B_{ij} = collection of second virial coefficients for ion pairs of unlike charge
C_{ij} = collection of third virial coefficients
C_P^o = standard-state heat capacity, kJ/mol·K
G^o = standard-state Gibbs free energy, kJ/mol
H^o = standard-state enthalpy, kJ/mol
I = ionic strength, Eq. 19
J = function defined by Eq. 32
K_{sp} = solubility product, such as Eq. 1
m_i = component molality, mol/kg
n = number of ions in solution
n_i = component moles, mol
p = number of regression parameters
R = universal gas constant, kJ/mol·K
S^o = standard-state entropy, J/mol·K
T = absolute temperature, K
T' = shifted temperature, Eqs. 39 and 40
w_w = mass of solvent (water), kg
x = dummy variable
z_i = ionic charge
Z = quantity defined by Eq. 22

Greek letters

α = parameter in Eq. 27
$\beta_{ij}^{(0)}$ = Pitzer parameter, Eq. 27
$\beta_{ij}^{(1)}$ = Pitzer parameter, Eq. 27
$\beta_{ij}^{(2)}$ = Pitzer parameter, Eq. 27
γ_i = component activity coefficient
θ_{ij} = interaction parameter
λ_{ij} = second virial coefficient, Eq. 18
μ_{ijk} = third virial coefficient, Eq. 18
ν = stoichiometric coefficient
Φ = objective function, Eq. 37
Φ_{ij} = collection of second virial coefficients for ion pairs of like charge
Ψ_{ijk} = collection of third virial coefficients

Subscripts and superscripts

app = apparent
f = formation reaction
fus = fusion (melting)
m = molality based
M = cation
o = standard state
r = reference
s = solid
sp = solubility product
T = temperature dependent
X = anion

Literature Cited

Berg, R. L., and C. E. Vanderzee, "Thermodynamics of Carbon Dioxide and Carbonic Acid: (a) The Standard Enthalpies of Solution of Na_2CO_3(s), $NaHCO_3$(s), and CO_2(g) in Water at 298.15 K; (b) The Standard Enthalpies of Formation, Standard Gibbs Energies of Formation, and Standard Entropies of CO_2(aq), HCO_3^-(aq), CO_3^{2-}(aq), $NaHCO_3$(s), Na_2CO_3(s), $Na_2CO_3 \cdot H_2O$(s), and $Na_2CO_3 \cdot 10H_2O$(s)," *J. Chem. Thermodyn.*, **10**, 1113 (1978).

Butler, J. N., and R. Huston, "Activity Coefficients and Ion Pairs in the Systems Sodium Chloride–Sodium Bicarbonate–Water and Sodium Chloride–Sodium Carbonate–Water," *J. Phys. Chem.*, **74**, 2976 (1970).

Chang, Y. A., and N. Ahmad, *Thermodynamic Data on Metal Carbonates and Related Oxides*, Metall. Soc. AIME, Amer. Inst. Min., Metall. and Petrol. Eng., New York (1982).

Chen, X., S. E. Gillespie, J. L. Oscarson, and R. M. Izatt, "Calorimetric Determination of Thermodynamic Quantities for Chemical Reactions in the System CO_2-NaOH-H_2O from 225 to 325°C," *J. Solution Chem.*, **21**, 825 (1992).

Cox, J. D., D. D. Wagman, and V. A. Medvedev, *CODATA Key Values for Thermodynamics*, Hemisphere, New York (1989).

Freeth, F. A., "II. The System: Na2O-CO_2-NaCl-H_2O, Considered as Two Four-Component Systems," *Roy. Soc. London Philos. Trans., Ser. A*, **A223**, 35 (1922).

Garrels, R. M., M. E. Thompson, and R. Siever, "Control of Carbonate Solubility by Carbonate Complexes," *Amer. J. Sci.*, **259**, 24 (1961).

Garrett, D. E., *Natural Soda Ash. Occurrences, Processing, and Use*, Van Nostrand Reinhold, New York (1992).

Greenberg, J. P., and N. Møller, "The Prediction of Solubilities in Natural Waters: A Chemical Equilibrium Model for the Na-K-Ca-Cl-SO_4-H_2O System to High Concentration from 0 to 250°C," *Geochim. Cosmochim. Acta*, **53**, 2503 (1989).

Grønvold, F., and K. K. Meisingset, "Thermodynamic Properties and Phase Transitions of Salt Hydrates Between 270 and 400 K II. $Na_2CO_3 \cdot H_2O$ and $Na_2CO_3 \cdot 10H_2O$," *J. Chem. Thermodyn.*, **15**, 881 (1983).

Harvie, C. E., N. Moller, and J. H. Weare, "The Prediction of Mineral Solubilities in Natural Waters: The Na-K-Mg-Ca-H-Cl-SO_4-OH-HCO_3-CO_3-CO_2-H_2O System to High Ionic Strengths at 25°C," *Geochim. Cosmochim. Acta*, **48**, 723 (1984).

Haynes, H. W., Jr., and P. De Filippis, "An Equation of State for Trona Solutions," *Proc. Int. Mineral Processing Congr.*, Rome, Italy (2000).

Helgeson, H. C., J. M. Delany, H. W. Nesbitt, and D. K. Bird, "Summary and Critique of the Thermodynamic Properties of Rock-Forming Minerals," *Amer. J. Sci.*, **278A**, 1 (1978).

Helgeson, H. C., D. H. Kirkham, and G. C. Flowers, "Theoretical Prediction of the Thermodynamic Behavior of Aqueous Electrolytes at High Pressures and Temperatures: IV. Calculation of Activity Coefficients, Osmotic Coefficients, and Apparent Molal and Standard and Relative Partial Molal Properties to 600°C and 5 kb," *Amer. J. Sci.*, **281**, 1249 (1981).

Hill, A. E., and L. R. Bacon, "Ternary Systems. VI. Sodium Carbonate, Sodium Bicarbonate and Water," *J. Amer. Chem. Soc.*, **49**, 2487 (1927).

Holmes, H. F., and R. E. Mesmer, "Thermodynamics of Aqueous Solutions of the Alkali Metal Sulfates," *J. Solution Chem.*, **15**, 495 (1986).

Keenan, J. H., and F. G. Keyes, *Thermodynamic Properties of Steam Including Data for the Liquid and Solid Phases*, Wiley, New York (1936).

Linke, W. F., *Solubilities. Inorganic and Metal-Organic Compounds*, Vol. II, 4th ed., Amer. Chem. Soc., Washington, DC (1965).

Møller, N., "The Prediction of Mineral Solubilities in Natural Waters: A Chemical Equilibrium Model for the Na-Ca-Cl-SO_4-H_2O System, to High Temperature and Concentration," *Geochim. Cosmochim. Acta*, **52**, 821 (1988).

Monnin, C., and J. Schott, "Determination of the Solubility Products of Sodium Carbonate Minerals and an Application to Trona Deposition in Lake Magadi (Kenya)," *Geochim. Cosmochim. Acta*, **48**, 571 (1984).

Nakayama, F. S., "Thermodynamic Functions for the Dissociation of $NaHCO_3^o$, $NaCO_3^-$, H_2CO_3 and HCO_3^-," *J. Inorg. Nucl. Chem.*, **33**, 1287 (1971).

Oelkers, E. H., H. C. Helgeson, E. L. Shock, D. A. Sverjensky, J. W. Johnson, and V. A. Pokrovskii, "Summary of the Apparent Standard Partial Molal Gibbs Free Energies of Formation of Aqueous Species, Minerals, and Gases at Pressures 1 to 5000 Bars and Temperatures 25 to 1000°C," *J. Phys. Chem. Ref. Data*, **24**, 1401 (1995).

Pabalan, R. T., and K. S. Pitzer, "Thermodynamics of Concentrated Electrolyte Mixtures and the Prediction of Mineral Solubilities to High Temperatures for Mixtures in the System Na-K-Mg-Cl-SO_4-OH-H_2O," *Geochim. Cosmochim. Acta*, **51**, 2429 (1987).

Pabalan, R. T., and K. S. Pitzer, "Heat Capacity and Other Thermodynamic Properties of Na_2SO_4(aq) in Hydrothermal Solutions and the Solubilities of Sodium Sulfate Minerals in the System Na-Cl-SO_4-OH-H_2O) to 300°C," *Geochim. Cosmochim. Acta*, **52**, 2393 (1988).

Peiper, J. C., and K. S. Pitzer, "Thermodynamics of Aqueous Carbonate Solutions Including Mixtures of Sodium Carbonate, Bicarbonate, and Chloride," *J. Chem. Thermodyn.*, **14**, 613 (1982).

Pitzer, K. S., J. C. Peiper, and R. H. Busey, "Thermodynamic Properties of Aqueous Sodium Chloride Solutions," *J. Phys. Chem. Ref. Data*, **13**, 1 (1984).

Pitzer, K. S., *Thermodynamics*, 3rd ed., McGraw-Hill, New York (1995).

Riggs, J. B., *An Introduction to Numerical Methods for Chemical Engineers*, Texas Tech Univ. Press, Lubbock, TX (1988).

Rogers, P. S. Z., and K. S. Pitzer, "Volumetric Properties of Aqueous Sodium Chloride Solutions," *J. Phys. Chem. Ref. Data*, **11**, 15 (1982).

Shock, E. L. and H. C. Helgeson, "Calculation of the Thermodynamic and Transport Properties of Aqueous Species at High Pressures and Temperatures: Correlation Algorithms for Ionic Species and Equation of State Predictions to 5 kb and 1000°C," *Geochim. Cosmochim. Acta*, **52**, 2009 (1988).

Shock, E. L., H. C. Helgeson, and D. A. Sverjensky, "Calculation of the Thermodynamic and Transport Properties of Aqueous Species at High Pressures and Temperatures: Standard Partial Molal Properties of Inorganic Neutral Species," *Geochim. Cosmochim. Acta*, **53**, 2157 (1989).

Tanger, J. C., IV, and H. C. Helgeson, "Calculation of the Thermodynamic and Transport Properties of Aqueous Species at High Pressures and Temperatures: Revised Equations of State for the Standard Partial Molal Properties of Ions and Electrolytes," *Amer. J. Sci.*, **288**, 19 (1988).

Tomaszewski, J., "Investigation of the Equilibrium of the System: Na_2CO_3-$NaHCO_3$-H_2O," *Stud. Soc. Sci. Torun., Sec. B*, **III**(2), 33 (1961).

Vanderzee, C. E., "Thermodynamic Relations and Equilibria in ($Na_2CO_3 + NaHCO_3 + H_2O$): Standard Gibbs Energies of Formation and Other Properties of Sodium Hydrogen Carbonate, Sodium Carbonate Heptahydrate, Sodium Carbonate Decahydrate, Trona: ($Na_2CO_3 \cdot NaHCO_3 \cdot 2H_2O$), and Wegscheider's Salt: ($Na_2CO_3 \cdot 3NaHCO_3$)," *J. Chem. Thermodyn.*, **14**, 219 (1982).

Waldeck, W. F., G. Lynn, and A. E. Hill, "Aqueous Solubility of Salts at High Temperatures. II. The Ternary System Na_2CO_3-$NaHCO_3$-H_2O from 100 to 200°," *J. Amer. Chem. Soc.*, **56**, 43 (1934).

Waterfield, C. G., R. G. Linford, B. B. Goalby, T. R. Bates, C. A. Elyard, and L. A. K. Staveley, "Thermodynamic Investigation of Disorder in the Hydrates of Sodium Carbonate," *Trans. Faraday Soc.*, **64**, 868 (1968).

Wegscheider, R., and J. Mehl, "Über Systeme Na_2CO_3-$NaHCO_3$-H_2O und das Existenzgebiet der Trona," *Monatsh. Chem. Verw. Teile Wiss.*, **49**, 283 (1928).

Manuscript received Aug. 1, 2002, and revision received Feb. 5, 2003.